Microscopic multiphonon approach to spectroscopy in the neutron-rich oxygen region

G. De Gregorio,[1,2] F. Knapp,[3] N. Lo Iudice,[2,4] and P. Veselý[1]
[1]*Nuclear Physics Institute, Czech Academy of Sciences, 250 68 Řež, Czech Republic*
[2]*INFN Sezione di Napoli, 80126 Napoli, Italy*
[3]*Faculty of Mathematics and Physics, Charles University, 116 36 Prague, Czech Republic*
[4]*Dipartimento di Fisica, Università di Napoli Federico II, 80126 Napoli, Italy*

(Received 20 November 2017; revised manuscript received 10 January 2018; published 8 March 2018)

Background: A fairly rich amount of experimental spectroscopic data have disclosed intriguing properties of the nuclei in the region of neutron rich oxygen isotopes up to the neutron dripline. They, therefore, represent a unique laboratory for studying the evolution of nuclear structure away from the stability line.
Purpose: We intend to give an exhaustive microscopic description of low and high energy spectra, dipole response, weak, and electromagnetic properties of the even ^{22}O and the odd ^{23}O and ^{23}F.
Method: An equation of motion phonon method generates an orthonormal basis of correlated n-phonon states ($n = 0,1,2,\dots$) built of constituent Tamm-Dancoff phonons. This basis is adopted to solve the full eigenvalue equations in even nuclei and to construct an orthonormal particle-core basis for the eigenvalue problem in odd nuclei. No approximations are involved and the Pauli principle is taken into full account. The method is adopted to perform self-consistent, parameter free, calculations using an optimized chiral nucleon-nucleon interaction in a space encompassing up to two-phonon basis states.
Results: The computed spectra in ^{22}O and ^{23}O and the dipole cross section in ^{22}O are in overall agreement with the experimental data. The calculation describes poorly the spectrum of ^{23}F.
Conclusions: The two-phonon configurations play a crucial role in the description of spectra and transitions. The large discrepancies concerning the spectra of ^{23}F are ultimately traced back to the large separation between the Hartree-Fock levels belonging to different major shells. We suggest that a more compact single particle spectrum is needed and can be generated by a new chiral potential which includes explicitly the contribution of the three-body forces.

DOI: 10.1103/PhysRevC.97.034311

I. INTRODUCTION

The region of the neutron rich oxygen isotopes has been explored extensively in several experimental and theoretical investigations. Intriguing properties have emerged from these studies.

Several experiments have produced a fairly rich amount of spectroscopic data which have provided evidence for the new magic numbers $N = 14$ and $N = 16$ and traced out the neutron dripline [1–15].

Radioactive beam experiments [16–18] have detected in the queue of the giant dipole resonance (GDR) bunches of peaks in ^{20}O and ^{22}O, exhausting 8%–10% of the energy weighted sum rule, in qualitative agreement with a shell model calculation [19], and tentatively associated to the pygmy dipole resonance (PDR). An analysis and a fairly complete list of references can be found in [20].

Several theoretical investigations have been devoted to this region. A shell model calculation used an empirical interaction and included the continuum [21], another stressed the important role of the three-body potential [22] in enforcing the $N = 16$ shell closure. Three-body forces were employed also within a self-consistent Green's function theory approach [23,24] and in a many-body perturbation theory calculation [25].

Several studies adopted the coupled cluster (CC) method. They were focused on bulk properties and low-energy levels [26–32]. Most of the CC numerical applications used $NN + 3N$ chiral forces derived from an effective field theory. One, in particular, studied the effect of the continuum and the three-body forces [31]. The CC method was also combined with a Lorentz integral transform to study the electric dipole response in this region [33].

Here, an exhaustive study of the spectroscopic properties of the even ^{22}O and the adjoining odd ^{23}O and ^{23}F is carried out within the equation of motion phonon method (EMPM).

The method was first formulated for even-even nuclei in the particle-hole (p-h) scheme [34–36] and, then, in terms of Hartree-Fock-Bogoliubov (HFB) quasiparticles (qp) [37]. It derives a set of equations yielding a basis of orthonormal multiphonon states, built of phonons obtained in Tamm-Dancoff approximation (TDA), and, then, solves the full eigenvalue problem in the space spanned by such a basis.

It was implemented numerically to describe the dipole response in heavy, neutron rich, nuclei [38–40], to study the full spectrum as well as the dipole response of the neutron rich ^{20}O [37], and to investigate the ground state correlations [41].

More recently, the method was extended to odd nuclei [42–44]. An orthonormal basis of states composed of a valence particle coupled to n-phonon states ($n = 0,1,2,\dots$), describing the excitations of a doubly magic core, is produced by a set of equations of motion and, then, employed for the solution of

the full eigenvalue problem. The method was applied to ^{17}O and ^{17}F and produced the complete level and decay schemes as well as the PDR and GDR cross sections.

In odd nuclei, the EMPM can be considered a generalization of the particle-vibration coupling (PVC) model [45] widely exploited in studies using the random-phase-approximation (RPA) and its extensions [46–55]. Many investigations exploited energy density functionals (EDF) derived from Skyrme forces [56–62] or based on the theory of finite Fermi systems [63], or deduced from relativistic meson-nucleon Lagrangians [64–67].

With respect to the mentioned approaches, the EMPM takes the Pauli principle into full account and does not rely on any approximation. It has, in fact, the same accuracy of shell model.

In our numerical implementation, we generate a HF basis from the chiral NN potential NNLO$_{\rm opt}$ determined in Ref. [68] by fixing the coupling constants at next-to-next leading order through a new optimization method in the analysis of the phase shifts, which minimizes the effects of the three-nucleon force.

This potential, while producing too much attraction in medium and heavy mass nuclei, reproduces well the experimental binding energies of light nuclei and oxygen isotopes. Thus, we will not add any corrective term as we did for heavy nuclei [40].

We then solve the eigenvalue problem for ^{22}O, considered as doubly magic, in a space encompassing up two-phonon states. The same n-phonon ($n = 0,1,2$) states are then coupled to the odd particle of the adjacent odd nuclei ^{23}O and ^{23}F to generate an orthonormal basis and solve the full eigenvalue problem. Complete level schemes as well as transition strengths and cross sections are produced and compared with the available experimental data. An analysis of the phonon composition of the states is performed in order to gain insights into the nature of levels and resonances.

II. EMPM FOR EVEN-EVEN NUCLEI

A. The eigenvalue problem

The method has been described in a previous paper [36]. Its primary goal is to generate an orthonormal basis of n-phonon correlated states

$$|\alpha_n\rangle = \sum_{\lambda\alpha_{n-1}} C^{\alpha_n}_{\lambda\alpha_{n-1}} |(\lambda \times \alpha_{n-1})^{\alpha_n}\rangle \tag{1}$$

of energy E_{α_n}, where

$$|(\lambda \times \alpha_{n-1})^{\alpha_n}\rangle = \{O^\dagger_\lambda \times |\alpha_{n-1}\rangle\}^{\alpha_n} \tag{2}$$

and

$$O^\dagger_\lambda = \sum_{\rm ph} c^\lambda_{\rm ph} (a^\dagger_p \times b_h)^\lambda \tag{3}$$

is the p-h TDA phonon operator of energy E_λ acting on the $(n-1)$-phonon basis states $|\alpha_{n-1}\rangle$, assumed to be known. The operators $a^\dagger_p = a^\dagger_{x_p j_p m_p}$ and $b_h = (-)^{j_h+m_h} a_{x_h j_h -m_h}$ create a particle and a hole of energies ϵ_p and $-\epsilon_h$, respectively.

As illustrated in Ref. [36], we start with the equations of motion

$$\langle\alpha_n\|[H, O^\dagger_\lambda]\|\alpha_{n-1}\rangle = (E_{\alpha_n} - E_{\alpha_{n-1}}) X^{\alpha_n}_{\lambda\alpha_{n-1}}, \tag{4}$$

where

$$\begin{aligned} X^{\alpha_n}_{\lambda\alpha_{n-1}} &= \langle\alpha_n\|O^\dagger_\lambda\|\alpha_{n-1}\rangle \\ &= [\alpha_n]^{1/2} \sum_{\lambda'\alpha'_{n-1}} \mathcal{D}^{\alpha_n}_{\lambda\alpha_{n-1}\lambda'\alpha'_{n-1}} C^{\alpha_n}_{\lambda'\alpha'_{n-1}}. \end{aligned} \tag{5}$$

Here, $[\alpha_n] = 2J_{\alpha_n} + 1$, a notation which will be used throughout the paper, and

$$\mathcal{D}^{\alpha_n}_{\lambda\alpha_{n-1}\lambda'\alpha'_{n-1}} = \langle(\lambda \times \alpha_{n-1})^\beta | (\lambda' \times \alpha'_{n-1})^\beta\rangle \tag{6}$$

is the overlap or metric matrix which reintroduces the exchange terms among different phonons and, therefore, re-establishes the Pauli principle.

After expanding the commutator, expressing the p-h operators in terms of the phonon operators $O^\dagger_\lambda$ upon inversion of Eq. (3), and exploiting Eq. (5), we obtain

$$\begin{aligned} &\sum_{\lambda_1\alpha_1\lambda'\alpha'} \left((E_\lambda + E_\alpha - E_{\alpha_n})\delta_{\lambda\lambda_1}\delta_{\alpha\alpha_1} + \mathcal{V}^{\alpha_n}_{\lambda\alpha\lambda_1\alpha_1}\right) \\ &\times \mathcal{D}^{\alpha_n}_{\lambda_1\alpha_1\lambda'\alpha'} C^{\alpha_n}_{\lambda'\alpha'} = 0, \end{aligned} \tag{7}$$

where α, α_1, and α' label $(n-1)$-phonon states. The expression of the $\mathcal{D}$ matrix and of the phonon-phonon potential $\mathcal{V}^{\alpha_n}_{\lambda\alpha\lambda_1\alpha_1}$ can be found in [36].

This is a generalized eigenvalue equation in the overcomplete basis $|(\lambda \times \alpha_{n-1})^{\alpha_n}\rangle$. Following the procedure outlined in Refs. [34,35], based on the Cholesky decomposition method, it is possible to extract a basis of linearly independent states spanning the physical subspace and obtain a non singular eigenvalue equation whose solution yields a basis of orthonormal correlated n-phonon states of the form (1).

Since recursive formulas hold for all quantities, it is possible to solve the eigenvalue equations iteratively starting from $n = 1$ (TDA phonons) and, thereby, generate a set of orthonormal multiphonon states $\{|0\rangle, |\alpha_1\rangle (= |\lambda\rangle), \ldots |\alpha_n\rangle \ldots\}$.

The basis $\{|\alpha_n\rangle\}$ is adopted to solve the eigenvalue equations in the multiphonon space

$$\sum_{n'\beta_{n'}} [(E_{\alpha_n} - \mathcal{E}_\nu)\delta_{nn'}\delta_{\alpha_n\beta_{n'}} + \mathcal{V}_{\alpha_n\beta_{n'}}] \mathcal{C}^{(\nu)}_{\beta_{n'}} = 0, \tag{8}$$

where the potential couples only n-phonon states belonging to subspaces differing by one or two phonons ($n' = n \pm 1$ and $n' = n \pm 2$).

The solution of Eq. (8) yields the final eigenvalues $\mathcal{E}_\nu$ and the corresponding eigenfunctions

$$|\Psi_\nu\rangle = \sum_{n\alpha_n} \mathcal{C}^{(\nu)}_{\alpha_n} |\alpha_n\rangle. \tag{9}$$

The entire procedure leading to these eigenstates does not rely on any approximation. Our approach, in fact, is equivalent to a large scale shell model in a space spanned by many p-h configurations.

Our method, however, offers an important advantage with respect to shell model. Since each n-phonon basis state spans the full np-nh subspace, it is possible to take into account the effect of high energy many p-h configurations even in a severely truncated multiphonon space. In shell model, instead, any cut of the basis implies the exclusion of some configurations.

$|\Psi_\nu\rangle$ can be written as a linear combination of products of n TDA phonons ($n = 0,1,2,3,\dots$). If the sum is truncated at $n = 2$, it assumes the form of a SRPA wave function [69–72] in its phonon version [73].

Thus, in a space encompassing up to two phonons, our formalism can be considered as the TDA counterpart of SRPA which incorporates effectively the ground state correlations. The underlying quasiboson approximation, however, produces uncontrollable uncertainties which induce instabilities [71,72].

B. Transition amplitudes

In the coupled scheme, the multipole operator has the structure

$$\mathcal{M}(\lambda\mu) = \frac{1}{[\lambda]^{1/2}} \sum_{rs} \langle r\|\mathcal{M}_\lambda\|s\rangle (a_r^\dagger \times b_s)^\lambda_\mu. \tag{10}$$

The reduced transition amplitudes are given by

$$\langle \Psi_{\nu'}\|\mathcal{M}(\lambda)\|\Psi_\nu\rangle = \sum_{(n\alpha_n)(n'\beta_{n'})} C^{(\nu)}_{\alpha_n} C^{(\nu')}_{\beta_{n'}} \langle \beta_{n'}\|\mathcal{M}(\lambda)\|\alpha_n\rangle. \tag{11}$$

The matrix elements of $\mathcal{M}(\lambda)$ between multiphonon states are

$$\begin{aligned}&\langle \beta_{n'}\|\mathcal{M}(\lambda)\|\alpha_n\rangle \\ &= [\lambda]^{-1/2}\Bigg[\delta_{n'n}\mathcal{M}^{(n)}_{\alpha\beta}(\lambda) + \sum_x \mathcal{M}(0\to x\lambda)\big(\delta_{n'(n+1)}X^{\beta_{n+1}}_{(x\lambda)\alpha_n} \\ &\quad +(-)^{\nu'-\nu}\delta_{n'(n-1)}X^{\alpha_n}_{(x\lambda)\beta_{n-1}}\big)\Bigg],\end{aligned} \tag{12}$$

where

$$\begin{aligned}\mathcal{M}(0\to x\lambda) &= \langle x\lambda\|\mathcal{M}(\lambda)\|0\rangle \\ &= \sum_{\rm ph} c^{(x\lambda)}_{\rm ph}\langle p\|\mathcal{M}(\lambda)\|h\rangle\end{aligned} \tag{13}$$

is the TDA transition amplitude and

$$\mathcal{M}^{(n)}_{\alpha\beta}(\lambda) = \sum_{rs}\langle r\|\mathcal{M}(\lambda)\|s\rangle \rho^{(n)}_{\alpha\beta}([r\times s]^\lambda) \tag{14}$$

the scattering term between states with the same number of phonons ($n' = n$). Here,

$$\rho^{(n)}_{\alpha\beta}([r\times s]^\sigma) = \langle \beta_n\|(a_r^\dagger \times b_s)^\sigma\|\alpha_n\rangle \tag{15}$$

is the density matrix and (rs) run over identical particles $(rs) = (\mathrm{pp}')$ and holes $(rs) = (\mathrm{hh}')$.

III. EIGENVALUE PROBLEM IN THE ODD NUCLEI

A. Generation of the basis

For a particle external to a doubly magic core we intend to generate the basis states of spin v

$$|\nu_n\rangle = \sum_{p\alpha_n} C^{\nu_n}_{p\alpha_n}|(p\times\alpha_n)^v\rangle = \sum_{p\alpha_n} C^{\nu_n}_{p\alpha_n}(a_p^\dagger \times |\alpha_n\rangle)^v, \tag{16}$$

where $|\alpha_n\rangle$ are the n-phonon core states (1).

In close analogy with the even nuclei we start with

$$\langle \alpha_n\|[b_p, H]^p\|\nu_n\rangle = (E_\nu - E_{\alpha_n})X^{(\nu_n)}_{p\alpha_n}, \tag{17}$$

where

$$X^{(\nu_n)}_{p\alpha_n} = \langle \alpha_n\|b_p\|\nu_n\rangle. \tag{18}$$

We will omit the subscript n when acting within a n-phonon subspace.

After expanding the commutator and inserting in X the expression (16) of $|\nu\rangle$, we obtain

$$\begin{aligned}&\sum_{p'\alpha' p_1\alpha_1}\big\{(\epsilon_p + E_\alpha - E_\nu)\delta_{pp'}\delta_{\alpha\alpha'} + \mathcal{V}^{(v)}_{p\alpha p'\alpha'}\big\} \\ &\times\mathcal{D}^{(v)}_{p'\alpha' p_1\alpha_1}C^{\nu}_{p_1\alpha_1} = 0.\end{aligned} \tag{19}$$

The particle-phonon interaction is

$$\mathcal{V}^{(v)}_{p\alpha p'\alpha'} = \sum_\sigma [\sigma]^{1/2} W(\alpha\sigma v p';\alpha' p)\mathcal{F}^\sigma_{p\alpha p'\alpha'} \tag{20}$$

and

$$\mathcal{F}^\sigma_{p\alpha p'\alpha'} = \sum_{tq} F^\sigma_{pp'tq}\rho_{\alpha'\alpha}([t\times q]^\sigma). \tag{21}$$

The overlap matrix is given by

$$\begin{aligned}\mathcal{D}^{(v)}_{p\alpha p'\alpha'} &= \langle (p'\times\alpha')^v|(p\times\alpha)^v\rangle \\ &= \delta_{pp'}\delta_{\alpha\alpha'} - (-)^{p-v+\alpha}\sum_\sigma [\sigma]^{1/2} W(p' p\alpha'\alpha;\sigma v) \\ &\quad\times\rho_{\alpha\alpha'}([p\times p']^\sigma).\end{aligned} \tag{22}$$

It reintroduces, through the density matrix ρ, the exchange terms among the odd particle and the n-phonon states and, therefore, re-establishes the Pauli principle.

Following the same Cholesky procedure adopted for the even-even nuclei we extract in each n subspace a basis of linearly independent states from the over-complete set $|(p\times\alpha_n)^v\rangle$ and obtain a nonsingular eigenvalue equation. Its iterative solution generates the particle-core correlated states $|\nu_n\rangle$ (16) of energies E_{ν_n} for $n = 1,2,\dots$ which, together with the single particle states $|\nu_0\rangle$, form an orthonormal basis.

B. Eigenvalue equations in the multiphonon basis

The basis $\{|\nu_0\rangle, |\nu_1\rangle, \dots |\nu_n\rangle \dots\}$ is employed to derive the eigenvalue equations

$$\sum_{\nu'_{n'}}\big\{(E_{\nu_n} - \mathcal{E}_\nu)\delta_{\nu_n\nu'_{n'}} + \mathcal{V}^{(v)}_{\nu_n\nu'_{n'}}\big\}\mathcal{C}^{(v)}_{\nu'_{n'}} = 0, \tag{23}$$

where $\mathcal{V}^{(v)}_{\nu_n\nu'_{n'}}$ is nonvanishing only for $n' \neq n$. We have for $n' = n+1$

$$\mathcal{V}^{(v)}_{\nu_n\nu'_{n+1}} = [v]^{-1/2}\sum_{(p\alpha_n)(p'\beta_{n+1})} C^{(\nu_n)}_{p\alpha_n}\mathcal{V}^{(v)}_{p\alpha_n p'\beta_{n+1}}X^{(\nu'_{n+1})}_{p'\beta_{n+1}}, \tag{24}$$

where

$$\begin{aligned}\mathcal{V}^{(v)}_{p\alpha_n p'\beta_{n+1}} &= \delta_{pp'}\langle\alpha_n|H|\beta_{n+1}\rangle \\ &\quad + \sum_\lambda [\lambda]^{1/2} W(\beta_{n+1}\lambda v p;\alpha_n p')\mathcal{F}^\lambda_{pp'}X^{(\beta_{n+1})}_{\lambda\alpha_n}\end{aligned} \tag{25}$$

and

$$\mathcal{F}^{\lambda}_{pp'} = \sum_{p_1h_1} F^{\lambda}_{pp'p_1h_1} c^{\lambda}_{p_1h_1}. \tag{26}$$

For $n' = n+2$ we get

$$\mathcal{V}^{(v)}_{\nu_n\nu'_{n+2}} = [v]^{-1/2} \sum_{p\alpha\beta_{n+2}} C^{(\nu_n)}_{p\alpha_n} \langle \alpha_n | H | \beta_{n+2} \rangle X^{(\nu'_{n+2})}_{p\beta_{n+2}}. \tag{27}$$

Equation (23) yields all the eigenvalues allowed by the space dimensions. The eigenfunctions have the structure

$$|\Psi_v\rangle = \sum_{\nu_n} \mathcal{C}^{v}_{\nu_n} |\nu_n\rangle, \tag{28}$$

where $|\nu_n\rangle$ is given by Eq. (16).

C. Transition amplitudes

Using the wave functions (28), we get the transition amplitudes

$$\langle \Psi_{v'} \| \mathcal{M}(\lambda) \| \Psi_v \rangle = \sum_{\nu_n\nu'_{n'}} \mathcal{C}^{v}_{\nu_n} \mathcal{C}^{v'}_{\nu'_{n'}} \langle \nu'_{n'} \| \mathcal{M}(\lambda) \| \nu_n \rangle, \tag{29}$$

where

$$\langle \nu'_{n'} \| \mathcal{M}(\lambda) \| \nu_n \rangle = [v]^{1/2} \sum_{p\alpha_n} C^{\nu_n}_{p\alpha_n} \mathcal{M}^{(\nu_n\nu'_{n'})}_{p\alpha_n}(\lambda). \tag{30}$$

For $n' = n$ we have

$$\begin{aligned} &\mathcal{M}^{(\nu_n\nu'_n)}_{p\alpha_n}(\lambda) \\ &= \sum_{p'} W(\lambda p' v \alpha_n; p v') \langle p' \| \mathcal{M}_\lambda \| p \rangle X^{(\nu'_n)}_{p'\alpha_n} \\ &\quad + \sum_{\alpha'_n} W(p\alpha_n v' \lambda p; v \alpha'_n) \langle \alpha'_n \| \mathcal{M}(\lambda) \| \alpha_n \rangle X^{(\nu'_n)}_{p\alpha'_n}. \end{aligned} \tag{31}$$

For $n' = n+1$ we get

$$\begin{aligned} \mathcal{M}^{(\nu_n\nu'_{n+1})}_{p\alpha_n}(\lambda) &= \sum_{\beta_{n+1}} W(\lambda\alpha_n v' p; \beta_{n+1} v) X^{(\nu'_{n+1})}_{p\beta_{n+1}} \\ &\quad \times \sum_{x} \mathcal{M}(0 \to [x\lambda]) X^{(\beta_{n+1})}_{(x\lambda)\alpha_n}. \end{aligned} \tag{32}$$

The transition amplitude for $n' = n-1$ can be deduced from the one for $n' = n+1$.

IV. NUMERICAL PROCEDURE AND RESULTS

A Hamiltonian composed of an intrinsic kinetic operator $T_{\rm int}$ plus the NN potential $V_{NN} = \mathrm{NNLO_{opt}}$ was employed to generate the HF basis in a space encompassing all harmonic oscillator shells up to $N_{\max} = 15$. A fraction (up to $N = 7$) of the HF states so obtained was used to determine the TDA phonon basis. We checked that the inclusion of higher energy shells does not affect the results.

We used all TDA phonons having dominant $0-\hbar\omega$ and $1-\hbar\omega$ components to generate the two-phonon basis.

The $J^\pi = 1^-$ TDA phonons are free of spurious admixtures induced by the center of mass (c.m.) motion. These spurious components have been removed by a method discussed in Ref. [74] based on the Gramm-Schmidt orthogonalization of the p-h basis to the c.m. state.

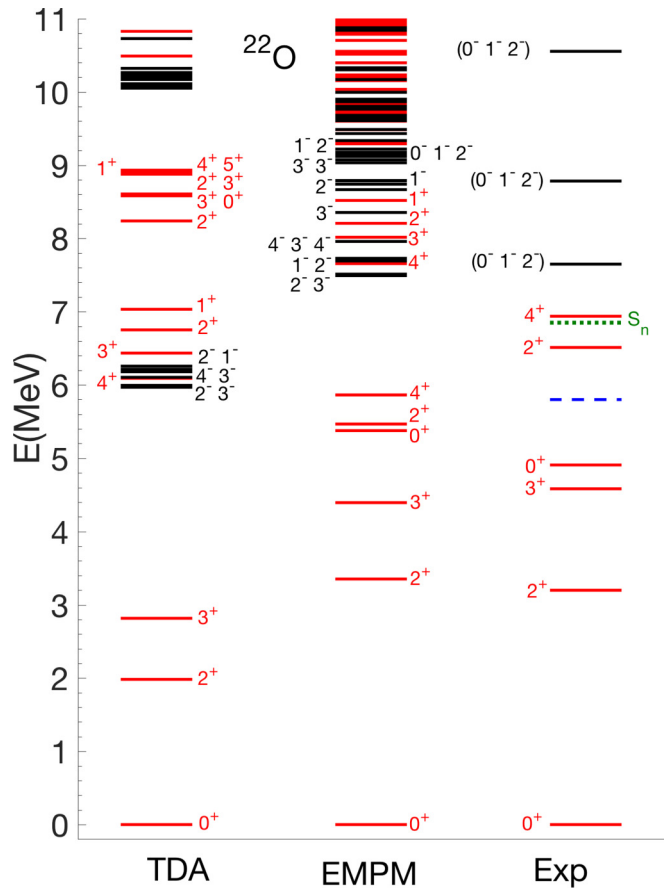

FIG. 1. Theoretical versus experimental [15] spectra of ^{22}O. The dashed line denotes a level of unknown spin and parity. The dotted line indicates the neutron decay threshold.

A. Spectra and phonon composition of the wave functions in ^{22}O

The theoretical spectra are compared to one another and with experiments [15] in Fig. 1. The inclusion of the two-phonon states reduces substantially the discrepancies with the experiments. We obtain a one to one correspondence between the computed low-lying positive parity levels and the bound experimental levels. The negative parity states are estimated to be above the neutron decay threshold consistently with experiments. In the continuum region the density of computed levels is very high.

As shown in Table I, the ground state is weakly correlated. The mixing of the HF vacuum with the two-phonon components is very modest. In fact, the two-phonon piece contributes with a small weight and is composed of a large number of two-phonon states of different multipolarity all having small amplitudes.

The excited states have an almost pure n-phonon character. The lowest 2^+_1 and 3^+_1 are practically pure TDA phonons and composed almost entirely of neutron p-h excitations, which account respectively for ∼99.5% and ∼ 99.8%. More specifically, they are determined by a single p-h excitation

TABLE I. Phonon composition of the low-lying states in ^{22}O.

J^π	E^ν	$\lvert C_0\rvert^2$	$\lvert C_1\rvert^2$	$\lvert C_2\rvert^2$
0_1^+	0.000	0.9142	0.0004	0.0854
2_1^+	3.352	0.0000	0.9305	0.0695
3_1^+	4.395	0.0000	0.9945	0.0055
0_2^+	5.377	0.0223	0.0011	0.9766
2_2^+	5.467	0.0000	0.0619	0.9381
4_1^+	5.863	0.0000	0.0003	0.9997
2_1^-	7.492	0.0000	0.9681	0.0319
3_1^-	7.512	0.0000	0.9726	0.0274
4_2^+	7.656	0.0000	0.9912	0.0088
2_2^-	7.693	0.0000	0.9603	0.0397
1_1^-	7.694	0.0000	0.9569	0.0431
4_1^-	7.695	0.0000	0.9699	0.0301
3_2^-	7.728	0.0000	0.9743	0.0257
4_2^-	7.959	0.0000	0.0254	0.9746
3_2^+	8.016	0.0000	0.9956	0.0044
2_3^+	8.206	0.0000	0.9660	0.0340
3_3^-	8.354	0.0000	0.0006	0.9994
1_1^+	8.518	0.0000	0.9605	0.0395
2_3^-	8.666	0.0000	0.0070	0.9930
3_4^-	8.740	0.0000	0.0094	0.9906
3_5^-	8.786	0.0000	0.0133	0.9867
1_2^-	8.790	0.0000	0.0090	0.9910
1_3^-	9.033	0.0000	0.0103	0.9897
2_4^-	9.075	0.0000	0.0144	0.9856
1_4^-	9.121	0.0000	0.0008	0.9992

within the (sd) shell (Table II). The large energy gap, especially for protons (∼28 MeV), inhibits the presence of $(1p)(0p)^{-1}$ configurations in these low-lying positive parity phonons.

The low-lying negative parity states have also a one-phonon nature and arise mainly from exciting a neutron from $0d_{5/2}$ to $1p_{1/2}$ or $1p_{3/2}$.

TABLE II. Energy ω_λ and p-h composition of selected TDA phonons of multipolarity λ in ^{22}O.

λ	ω_λ	$(p(h)^{-1})_\pi$	C^π	$(p(h)^{-1})_\nu$	C^ν
2_1^+	1.982			$1s_{1/2}(0d_{5/2})^{-1}$	−0.9974
2_2^+	6.752			$0d_{3/2}(0d_{5/2})^{-1}$	0.9894
3_1^+	2.816			$1s_{1/2}(0d_{5/2})^{-1}$	−0.9974
1_1^-	6.257	$0d_{5/2}(0p_{3/2})^{-1}$	0.1118	$1p_{3/2}(0d_{5/2})^{-1}$	0.9539
				$0f_{7/2}(0d_{5/2})^{-1}$	−0.1489
2_1^-	5.995			$1p_{3/2}(0d_{5/2})^{-1}$	−0.8324
				$1p_{1/2}(0d_{5/2})^{-1}$	0.5541
2_2^-	6.213			$1p_{3/2}(0d_{5/2})^{-1}$	0.5529
				$1p_{1/2}(0d_{5/2})^{-1}$	0.8311
3_1^-	5.968			$1p_{3/2}(0d_{5/2})^{-1}$	−0.9435
				$1p_{1/2}(0d_{5/2})^{-1}$	0.3304
3_2^-	6.180			$1p_{3/2}(0d_{5/2})^{-1}$	0.5529
				$1p_{1/2}(0d_{5/2})^{-1}$	0.9433

TABLE III. Weights $W_{\lambda\lambda'}$ (%) of the two-phonon components of selected states in ^{22}O.

J^π	E^ν	λ	λ'	$W_{\lambda\lambda'}$
0_1^+	0.000	1_1^+	1_1^+	0.46
		2_1^+	2_1^+	1.67
		2_1^+	2_2^+	0.84
		2_2^+	2_2^+	0.55
		3_1^+	3_1^+	0.87
		3_1^+	3_2^+	0.47
		3_2^+	3_2^+	0.75
		4_1^+	4_1^+	0.57
		1_1^-	1_1^-	0.19
0_2^+	5.377	2_1^+	2_1^+	63.98
		3_1^+	3_1^+	32.13
2_2^+	5.466	2_1^+	2_1^+	49.10
		2_1^+	3_1^+	19.50
		3_1^+	3_1^+	24.05
4_1^+	5.863	2_1^+	2_1^+	20.55
		2_1^+	3_1^+	71.81
		3_1^+	3_1^+	6.85

Above the 2_1^+ and 3_1^+ levels, we observe a $\{0_2^+,2_2^+,4_1^+\}$ two-phonon triplet. In order to get a better insight into the structure of these two-phonon states, we have evaluated the weight of their constituent phonons. Such a weight is obtained by expanding in terms of n-phonon components the normalization condition

$$\langle\Psi_\nu|\Psi_\nu\rangle = \sum_{\lambda\lambda'} W^\nu_{\lambda\lambda'} = 1 \tag{33}$$

obtaining

$$W^\nu_{\lambda\lambda'} = \sum_\alpha \frac{1}{[\alpha]^{1/2}} |\mathcal{C}^\nu_\alpha|^2 X^\alpha_{\lambda\lambda'}. \tag{34}$$

As shown in Table III, all the states of the $\{0_2^+,2_2^+,4_1^+\}$ two-phonon triplet are composed of the low-lying 2_1^+ and 3_1^+ phonons and therefore have a neutron nature. Their alike phonon composition suggests that this triplet has in part an harmonic character.

To further check this conjecture we have computed the isoscalar (IS) $E\lambda = E2$ reduced transition strengths

$$B_{\rm IS}(E\lambda; J_i^\pi \to J_f^\pi) = \frac{1}{[J_i]} |\langle J_f^\pi \| \mathcal{M}_{\rm IS}(E\lambda) \| J_i^\pi\rangle|^2 \tag{35}$$

using the isoscalar component of the $\lambda = 2$ operator

$$\mathcal{M}(E\lambda\mu) = \frac{1}{2} e \sum_i (1 - \tau_3(i)) r_i^\lambda Y_{\lambda\mu}(\hat{r}_i), \tag{36}$$

where $\tau_3 = 1$ for neutrons and $\tau_3 = -1$ for protons.

We obtain $B_{\rm IS}(E2; 2_1^+ \to 0_1^+) = 4.07$ $(e^2{\rm fm}^4)$ and $B_{\rm IS}(E2; J_i^\pi \to 2_1^+) = 6.40,\ 4.22,\ 8.01$ $(e^2{\rm fm}^4)$ for $J_i^\pi = 0_2^+,\ 2_2^+,\ 4_1^+$, respectively. These values support with good approximation the harmonic character of the spectrum.

It is to be stressed, however, that the harmonicity predicted by the calculation seems to be supported only partially by

the experimental spectrum. While, in fact, the theoretical $\{0_2^+, 2_2^+, 4_1^+\}$ levels are close together, the measured 0_2^+ level is quite lower than the other two members of the triplet.

The harmonic character of the computed spectrum can be easily understood. Since the low-lying TDA phonons arise almost entirely from the excitations of the $0d_{5/2}$ neutrons, the mixing among the different low-energy n-phonon subspaces is ruled only by the weak neutron-neutron interaction between a small fraction of neutrons.

Only if neutron and, especially, proton p-h excitations involving $0p$ shells occur with appreciable amplitudes in these low-lying phonons, the full NN interaction would be active among all nucleons and would be effective in the coupling among different n-phonon components thereby enhancing their mixing.

A larger proton p-h content of the low-lying phonons would enhance the ground state $E2$ strength which now is estimated to be too small. Using, in fact, the full $E2$ operator (29), which has bare charges, we obtain $B(E2; 0_1^+ \to 2_1^+) = 0.28$ $e^2\text{fm}^4$. This value, which comes entirely from protons, is two orders of magnitude smaller than the experimental strength $B_{\text{exp}}(E2; 0_1^+ \to 2_1^+) = 21 \pm 8\ e^2\text{fm}^4$ determined via inelastic scattering of a ^{22}O radioactive beam from ^{197}Au [1]. The strength is, instead, fairly well reproduced in two HFB plus RPA approaches using Skyrme [75] and Gogny [76] forces. These forces are devised so as to reproduce the bulk properties at the HF(B) level, which is not our case. In fact, the HF calculation using the optimized NNLO$_{\text{opt}}$ yields only half-binding energy [41]. The good agreement achieved in the mentioned RPA approaches suggests that the 2^+ state has a much larger proton content than the one obtained here.

B. Dipole response in ^{22}O

The total dipole cross section is given by

$$\sigma(E1) = \int_0^\infty \sigma(E1,\omega)d\omega = \frac{16\pi^3}{9\hbar c}\int_0^\infty \omega \mathcal{S}(E1,\omega)d\omega, \tag{37}$$

where $\mathcal{S}(E1,\omega)$ is the strength function

$$\mathcal{S}(E1,\omega) = \sum_\nu B_\nu(E1)\,\delta(\omega - \omega_\nu) \tag{38}$$

and $B_\nu(E1) = B(E1; 0_1^+ \to \nu)$ the reduced strength of the transition to the ν_{th} final state of energy $\omega_\nu = \mathcal{E}_\nu - \mathcal{E}_0$.

The total cross section $\sigma(E1)$ is proportional to the energy weighted sum

$$\sigma(E1) = \frac{16\pi^3}{9\hbar c}\sum_\nu \omega_\nu B_\nu(E1) \tag{39}$$

and satisfies the Thomas-Reiche-Kuhn (TRK) sum rule if the Hamiltonian does not contain momentum dependent and exchange terms.

The reduced strength $B_\nu(E1)$ is computed using the operator with bare charges [Eq. (29)]. Moreover, the δ function is replaced by a Lorentzian with smearing width Δ in the calculation of $\sigma(E1,\omega)$.

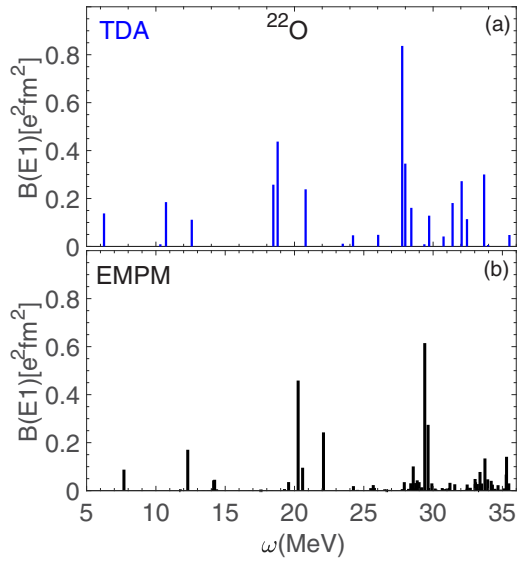

FIG. 2. TDA (a) and EMPM (b) $E1$ reduced strength distributions in ^{22}O.

We have also computed the isoscalar reduced strength $B_\nu(E1, IS)$ using the operator

$$\mathcal{M}_{\text{IS}}(E1\mu) = e\sum_{i=1}^{A}\left(r_i^3 - \frac{5}{3}\langle r^2\rangle r_i\right)Y_{1\mu}(\hat{r}_i), \tag{40}$$

where the second term in the bracket is meant to remove partially the contribution of the center of mass. Such a term does not contribute in our case since our TDA states are free of center of mass spurious admixtures.

The IS strengths satisfy the energy weighted sum rule

$$\sum_\nu \omega_\nu B_\nu(E1, IS) = \frac{3}{16\pi}\frac{\hbar^2}{2m}A(11\langle r^4\rangle - 10R^2\langle r^3\rangle + 3R^4), \tag{41}$$

where

$$\langle r^n\rangle = \frac{3}{3+n}R^n \tag{42}$$

and $R = 1.2A^{1/3}$ fm.

In both TDA [Fig. 2(a)] and EMPM [Fig. 2(b)], the isovector $E1$ strength is distributed in the interval ∼7–35 MeV (Fig. 2) with a large concentration in the energy interval ∼26–35 MeV where no experimental data are available. The EMPM spectrum is more fragmented due to the damping action of the one-phonon to two-phonon coupling. Such a coupling is practically ineffective at low energy where the states have a pure one-phonon character.

The cross section is shifted upward by ∼2 MeV by the phonon coupling but keeps basically its shape (Fig. 3). It follows qualitatively the trend of the data deduced from electromagnetic dissociation cross sections [16] in the energy range ∼7–25 MeV and exhibits the highest peak around 30 MeV.

The summed cross sections up ∼21 MeV and ∼25 MeV exhaust, respectively, ∼19% and ∼30% of the TRK sum rule. Both fractions are within the errors of the experimental sums.

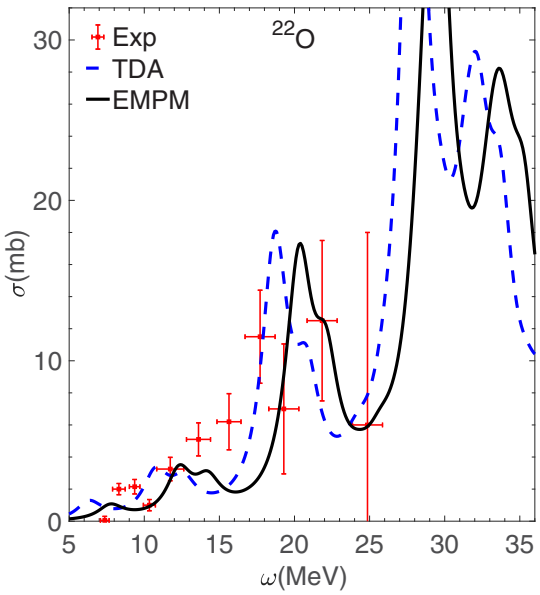

FIG. 3. Theoretical versus experimental [16] $E1$ cross section in ^{22}O. A Lorentzian of width $\Delta = 2$ MeV is used.

The largest contribution comes from the strength at higher energy. In fact, the total sum up to ∼40 MeV accounts for ∼125%.

The upward energy displacement of the theoretical cross section with respect to the data seems to confirm the suggestion that the HF proton p-h energy separation is too large. In this specific case the gap between the proton (sd) and $(0p)$ shells is ∼22 MeV.

The strength in the interval ∼7–15 MeV is generated by $E1$ transitions (Fig. 2) to states having dominant neutron character (Table III). These states, in fact, are excited by both the isovector and isoscalar probes (Fig. 4) and, therefore, may be associated to the PDR.

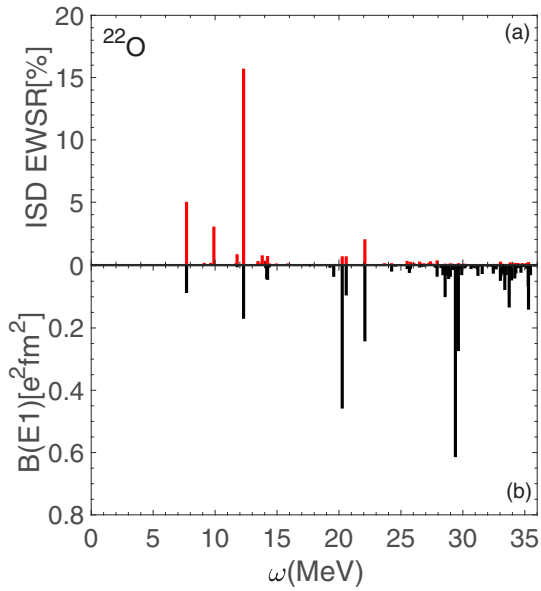

FIG. 4. Isoscalar (a) versus isovector (b) $E1$ transitions.

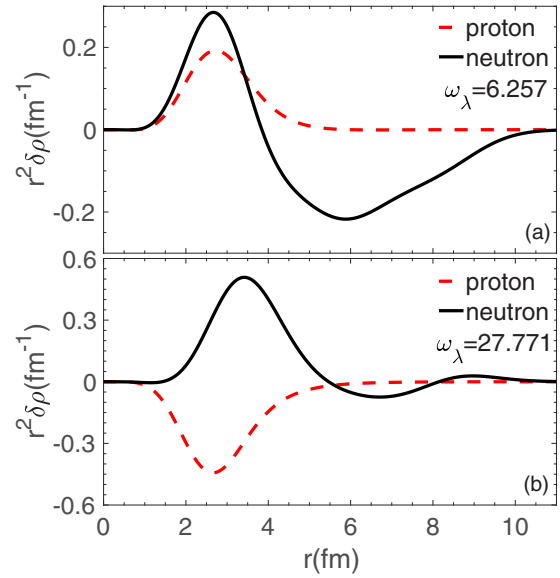

FIG. 5. Transition densities for the low-lying 1^-_1 state (a) and one falling in the region of the GDR (b).

Such a conjecture is supported by the trend of the transition densities. The neutron skin oscillates against the core at low energy [Fig. 5(a)] while proton and neutron fluids oscillate in opposition of phases at high energy [Fig. 5(b)].

C. Spectra and wave functions in ^{23}O and ^{23}F

The spectrum of ^{23}O determined experimentally [13] is composed of two positive parity $5/2^+$ and $3/2^+$ levels and a level at higher energy probably of negative parity (Fig. 6). All of them are above the neutron decay threshold.

The computed levels are also above such a threshold. Those of positive parity are close in energy to the corresponding experimental levels. The calculation yields also negative parity levels compatible in spin and energy with the experimental one [13]. The overall agreement with experiments is achieved only once the phonons are included.

As in ^{22}O, all the states have substantially a single n-phonon structure (Table IV). The $3/2^+_1$ as well as the lowest negative parity states have a single particle nature. The first excited state $5/2^+_1$, instead, is basically a particle-phonon state (Table IV) resulting mainly from coupling the $1/2^+_1$ particle to the 3^+_1 phonon. This component accounts for ∼97% of the total wave function.

The calculation yields a quintuplet of positive parity states $\{1/2^+_2, 3/2^+_2, 5/2^+_2, 7/2^+_1, 9/2^+_1\}$ in the energy interval ∼4.8–6.2 MeV (Fig. 6 and Table IV). They are built by coupling the $1/2^+_1$ neutron particle to the low-lying two-phonon triplet $\{0^+_2, 2^+_2, 4^+_1\}$ occurring in ^{22}O (Fig. 1).

Thus, the computed ^{23}O level scheme keeps memory of the harmonic nature of the spectrum predicted, but only partially confirmed experimentally, for the ^{22}O. Indeed, the particle-phonon coupling $\mathcal{F}^{\lambda'}_{pp'}$ (26) between the valence neutron and the low-lying phonons entering the matrix elements (24) between states differing by one-phonon is practically ineffective, given the neutron nature of these phonons. In fact the neutron-neutron

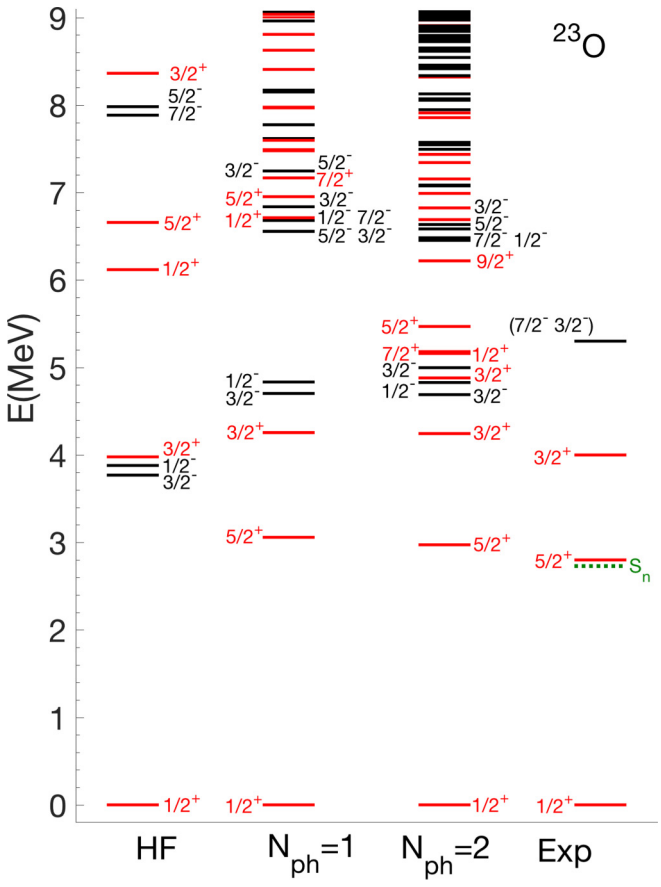

FIG. 6. Level schemes of ^{23}O computed in HF and in spaces including up to $N_{ph} = 1$ and $N_{ph} = 2$ phonons. The experimental data are from [13].

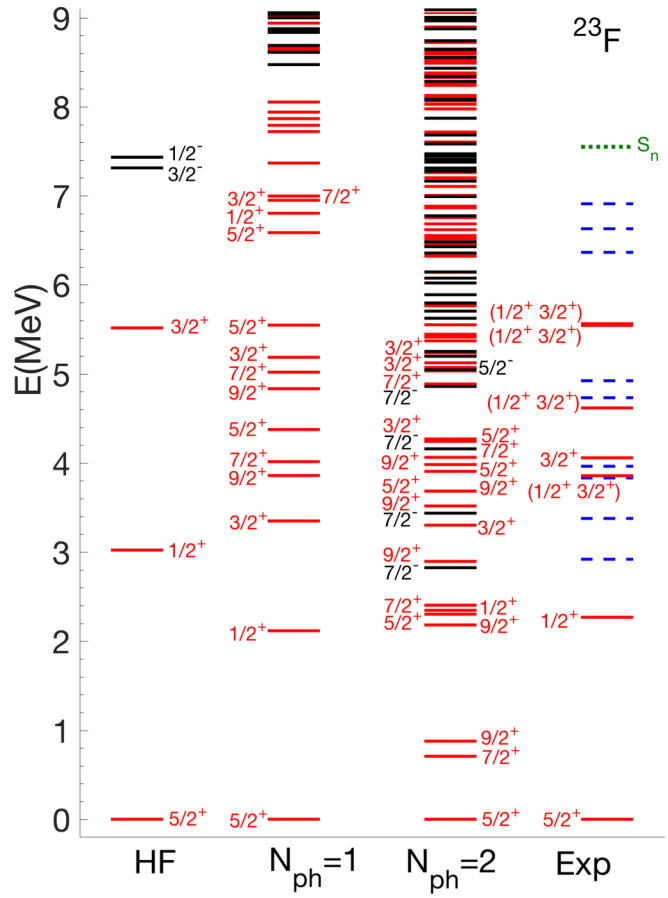

FIG. 7. Level schemes of ^{23}F computed in HF and in spaces including up to $N_{ph} = 1$ and $N_{ph} = 2$ phonons. The experimental data are from [5,6].

interaction is weak and acts among the few neutrons in excess. Moreover, the Pauli principle exerts an inhibiting action.

The experimental spectrum of ^{23}F [5,6] is much richer compared to ^{23}O and cannot be described satisfactorily in HF (Fig. 7). As the one-phonon components are included, several new levels occur at low energy and, up to the neutron decay threshold, are comparable in number with the levels detected experimentally. In addition to the low energy $1/2^+_1$ and $3/2^+_1$ levels which have an experimental counterpart, several $\{3/2^+,5/2^+,7/2^+,9/2^+\}$ levels occur in the region of experimental observation. Levels of the same spins were predicted also by shell model calculations using phenomenological two-body forces [5].

TABLE IV. Phonon composition of the low-lying states in ^{23}O.

J^π	E^ν	$\lvert C_0\rvert^2$	$\lvert C_1\rvert^2$	$\lvert C_2\rvert^2$
$1/2^+_1$	0.000	0.9404	0.0594	0.0002
$5/2^+_1$	2.973	0.0003	0.9948	0.0049
$3/2^+_1$	4.244	0.9507	0.0478	0.0015
$3/2^-_1$	4.688	0.9049	0.0905	0.0046
$1/2^-_1$	4.827	0.9686	0.0307	0.0007
$3/2^+_2$	4.880	0.0000	0.0000	1.0000
$3/2^-_2$	4.996	0.0498	0.8645	0.0852
$7/2^+_1$	5.159	0.0000	0.0000	1.0000
$1/2^+_2$	5.181	0.0000	0.0000	1.0000
$5/2^+_2$	5.468	0.0000	0.0000	1.0000
$9/2^+_1$	6.218	0.0000	0.0000	1.0000
$7/2^-_1$	6.452	0.0095	0.9374	0.0531
$5/2^-_1$	6.482	0.0004	0.9924	0.0072
$1/2^-_2$	6.583	0.0011	0.9930	0.0059
$3/2^-_3$	6.633	0.0284	0.9656	0.0060

The inclusion of two-phonons, while improving the agreement of the $1/2^+_1$ and $3/2^+_1$ levels with experiments, enhances dramatically the level density and pushes some of the high spin states very low in energy. Thus, the agreement with the experiments, achieved qualitatively by including only the one-phonon states, is spoiled.

The too strong proton-phonon coupling $\mathcal{F}^{\lambda'}_{pp'}$ (26) is responsible for this unwanted effect. Such a coupling not only admixes strongly particle and particle-phonon states but also one-phonon and two-phonon particle-core states through the matrix elements (24) (Table V). Why such a coupling is so strong can be easily understood. The p-h constituents of the low-lying phonons arise entirely from the excitations of $0d_{5/2}$ neutrons (Table III). The coupling, therefore, is strong since the proton-neutron interaction is strongly attractive and, also, because the Pauli principle is ineffective.

TABLE V. Phonon composition of selected states in ^{23}F.

J^π	E^ν	$\lvert C_0\rvert^2$	$\lvert C_1\rvert^2$	$\lvert C_2\rvert^2$
$5/2^+_1$	0.000	0.7188	0.2035	0.0777
$7/2^+_1$	0.707	0.0000	0.7474	0.2526
$9/2^+_1$	0.877	0.0001	0.7614	0.2385
$9/2^+_2$	2.182	0.0003	0.7044	0.2953
$5/2^+_2$	2.303	0.0564	0.7191	0.2245
$1/2^+_1$	2.346	0.6959	0.2531	0.0510
$7/2^+_2$	2.403	0.0000	0.7661	0.2339
$7/2^-_1$	2.825	0.0003	0.3766	0.6231
$9/2^+_3$	2.895	0.0000	0.4137	0.5863
$3/2^+_1$	3.302	0.4608	0.4742	0.0650
$7/2^-_2$	3.437	0.0000	0.3595	0.6405
$9/2^+_4$	3.518	0.0000	0.3248	0.6752
$5/2^+_3$	3.683	0.0055	0.7503	0.2442
$9/2^+_5$	3.685	0.0000	0.3287	0.6713
$3/2^+_2$	4.160	0.0251	0.8320	0.1429
$3/2^+_3$	5.445	0.0013	0.6509	0.3478
$3/2^+_4$	5.776	0.1180	0.6762	0.2058
$1/2^+_2$	6.322	0.0442	0.6402	0.3156
$3/2^+_5$	7.451	0.0281	0.7252	0.2467
$1/2^+_3$	7.454	0.0028	0.2242	0.7730
$1/2^+_4$	8.028	0.0937	0.8387	0.0676

This serious discrepancy with the experiments claims once again a quenching of the amplitudes of the TDA p-h configurations generated by the $0d_{5/2}$ neutron excitations in favor of components of higher energy.

D. β decay of ^{23}O

The experiments on the β decay of ^{23}O have detected six allowed decays to excited states of spin $1/2^+$ or $3/2^+$ in ^{23}F [6]. It is therefore useful to perform a theoretical investigation of the these decays based on our method. We need therefore to compute the ft value

$$ft_{1/2} = \frac{\kappa}{B(F) + B(GT)}, \tag{43}$$

where $\kappa = 6146$ s. The reduced strengths are

$$B(\lambda; \nu \to \nu') = \frac{1}{[\nu]} |\langle \nu' \| \mathcal{M}(\lambda) \| \nu \rangle|^2, \tag{44}$$

where $\mathcal{M}(\lambda)$ is either $\mathcal{M}_F$ or $\mathcal{M}_{GT}$ and

$$\mathcal{M}_F = g_V \sum_k t_+(k), \tag{45}$$

$$\mathcal{M}_{GT} = g_A \sum_k t_+(k) \vec{\sigma}(k). \tag{46}$$

We have introduced the spherical components t_μ of the isospin single particle operator and used the bare weak charges $g_v = 1$ and $g_A = 1.25$.

Since the contribution from the two-phonon components can be neglected in our case, the transition amplitude (29) can be written

$$\langle \Psi_{\nu'} \| \mathcal{M}_\lambda \| \Psi_{1/2^+_1} \rangle \simeq \mathcal{M}^{\nu\nu'}_{00}(\lambda) + \mathcal{M}^{\nu\nu'}_{01}(\lambda) + \mathcal{M}^{\nu\nu'}_{10}(\lambda) + \mathcal{M}^{\nu\nu'}_{11}(\lambda), \tag{47}$$

where ν' denotes all final states of spin and parity $\nu' = 1/2^+$ or $\nu' = 3/2^+$.

The single particle amplitudes are given by

$$\mathcal{M}^{\nu\nu'}_{00}(\lambda) = \sum_{ik} \mathcal{C}^{\nu}_{\nu_i} \mathcal{C}^{\nu'}_{\nu'_k} \langle \nu'_k \| \mathcal{M}_\lambda \| \nu_i \rangle. \tag{48}$$

The particle-phonon transition amplitudes are

$$\mathcal{M}^{\nu\nu'}_{01}(\lambda) = \sum_{p'h} \langle p' \| \mathcal{M}_\lambda \| h \rangle W^{\nu\nu'}_{hp'}(\lambda), \tag{49}$$

where

$$W^{\nu\nu'}_{hp'}(\lambda) = -\sum_{i\nu'_1} C^{\nu}_{\nu_i} C^{\nu'}_{\nu'_1} \times \sum_\sigma [\sigma]^{1/2} W(p'\lambda\sigma\nu; h\nu') c^{\sigma}_{\nu_i h}(\pi) \langle \sigma \| b_{p'} \| \nu'_1 \rangle. \tag{50}$$

$\mathcal{M}_{10}(\lambda)$ is deduced easily from $\mathcal{M}_{01}(\lambda)$.

The phonon-phonon amplitudes are

$$\mathcal{M}^{\nu\nu'}_{11}(\lambda) = \sum_{pp'} \langle p'_\nu \| \mathcal{M}_\lambda \| p_\pi \rangle W^{\nu\nu'}_{pp'}(\lambda), \tag{51}$$

where

$$W^{\nu\nu'}_{pp'}(\lambda) = \sum_{\nu_1\nu'_1\sigma} \mathcal{C}^{\nu}_{\nu_1} C^{\nu'}_{\nu'_1} (-)^{\nu'+p-\lambda-\sigma} [\sigma]^{1/2} W(\nu' p' \nu p; \sigma\lambda) \times \langle \sigma \| b_{p'} \| \nu'_1 \rangle \langle \sigma \| b_p \| \nu_1 \rangle. \tag{52}$$

HF yields only two $1/2^+$ states below $\sim$11 MeV (Fig. 7). The number of states populated by the decay increases substantially once the phonons are included (Table VI). Just six of them have energies comparable to the six levels populated in the experiment.

The *ft* values of several decays are comparable with the experimental data (Table VI). The strength of the GT transitions to the states ν' of spin 3/2 are comparable with those deduced from the data or one order of magnitude larger. Such a large contribution comes from the particle-phonon piece $\mathcal{M}_{01}(GT)$ [Eq. (49)] and is due to the large single particle coefficients of the initial state $1/2^+_1$ and to the large amplitudes $\langle \sigma \| b_{p'} \| \nu'_1 \rangle$ ($p' = 0d_{5/2}$ and $\nu'_1 = 3/2^+_i$) in Eq. (50) since the low-lying $|\nu'_1\rangle$ states are composed dominantly of a $0d_{5/2}$ proton coupled to a single one-phonon core state.

The GT contribution is also dominant in the transitions to the $1/2^+_i$ states with one remarkable exception, the $1/2^+_1 \to 1/2^+_4$ transition whose Fermi contribution is overwhelmingly large [$B(F) = 7.36$]. It comes from the particle-phonon transition $\mathcal{M}_{01}(F)$ [Eq. (49)] and is the result of several combined effects: i) The large overlap between the proton and neutron single particle states [$\langle p' \| \mathcal{M}_F \| h \rangle = \sqrt{6} \langle (0d_{5/2})_\pi | (0d_{5/2})_\nu \rangle$ in Eq. (49)], ii) the large amplitude $\langle \sigma \| b_{p'} \| \nu'_1 \rangle$ ($p' = 0d_{5/2}$ and $\nu'_1 = 1/2^+_4$), iii) the dominance of the $[1s_{1/2} \times (0d_{5/2})^{-1}]$ in several phonons σ.

A smaller single particle amplitude of the ^{23}O $1/2^+_1$ in favor of its one-phonon components would reduce i) the

TABLE VI. log(*ft*) values and GT reduced strengths of the ground state decay of ^{23}O.

Theory				
ν_f	ω_f	log (*ft*)	$B(F)$	B(GT)
$1/2_1^+$	2.346	3.95	0.03	0.658
$3/2_1^+$	3.302	5.20	0.0	0.038
$3/2_2^+$	4.160	4.67	0.0	0.13
$3/2_3^+$	5.445	3.94	0.0	0.69
$3/2_4^+$	5.776	3.61	0.0	1.48
$1/2_2^+$	6.322	3.51	0.30	1.61
$3/2_5^+$	7.451	8.17	0.0	0.00004
$1/2_3^+$	7.454	4.52	0.03	0.154
$1/2_4^+$	8.028	2.91	7.36	018
$3/2_6^+$	8.127	3.96	0.0	0.67
$3/2_7^+$	8.328	4.46	0.0	0.21
$1/2_5^+$	9.233	5.24	0.03	0.003
$1/2_6^+$	9.413	3.86	0.07	0.77
$1/2_7^+$	10.699	4.80	0.02	0.08
$1/2_8^+$	11.003	4.12	0.03	0.43
Experiments [6]				
ν_f		ω_f	log(*ft*)	B(GT)
$1/2^+$		2.243	4.27	0.32
$(1/2^+,3/2^+)$		3.866	4.33	0.29
$3/2^+$		4.066	4.24	0.36
$(1/2^+,3/2^+)$		4.604	4.82	0.09
$(1/2^+,3/2^+)$		5.553	4.68	0.13
$(1/2^+,3/2^+)$		5.559	4.28	0.32

strength of the transition between the states having single particle character, ii) the dominant particle-phonon contribution $\mathcal{M}_{01}(GT; 1/2_1^+ \rightarrow 3/2_i)$ transition, ii) the anomalously large strength of the Fermi transition to the $1/2_4^+$ state. Once again, such a result can be achieved if the amplitudes of the high energy p-h configurations in the TDA phonons are enhanced at the expenses of the too dominant low-lying p-h neutron components.

V. CONCLUDING REMARKS

The analysis of the results has pointed out the strong impact of the phonon states on spectra, dipole responses and β-decay transitions. This impact is especially positive in ^{22}O and ^{23}O. In ^{22}O, the two-phonon states are the main ingredients of a triplet of levels observed experimentally and, through their coupling, bring the one-phonon level close to the experimental one. In ^{23}O, a satisfactory agreement with the available experimental levels is reached only once the one and two-phonon states are included.

The impact on ^{23}F is less positive. In fact, because of the strong coupling between the odd proton and the phonons, several multiplets of states, arising from coupling the proton to the low-lying 2_1^+ and 3_1^+ phonons, are pushed down in energy thereby enhancing greatly the level density of the low-energy region of the spectrum. Moreover, few of these intruders fall at too low energy.

The origin of such a strong proton-phonon coupling resides in the dominance of the p-h configurations arising from the excitations of the $0d_{5/2}$ neutrons in all low-lying phonons. One of the effects of such a neutron dominance is to amplify the action of the strong proton-neutron interaction. It is therefore necessary to reduce the weight of the low-lying neutron p-h configurations in favor of neutron and proton p-h components of higher energy.

A more moderate dominance of the low-lying neutron p-h states in favor of protons would improve further the spectra of ^{22}O and ^{23}O by partly breaking their too harmonic character and would enhance the $B(E2)$ strength in ^{22}O, now badly underestimated. It would reduce the single particle amplitude of the $1/2_1^+$ state of ^{23}O and, therefore, would promote the quenching of some β-decay transitions. On the other hand, a larger phonon content of the same ^{23}O $1/2_1^+$ state would enhance the strengths of the other transitions which involve the one-phonon components.

The recipe for achieving such a goal is to generate more compact HF spectra. The HF levels belonging to the (sd) and $1p$ shells are very far apart from the $0p$ levels. For instance, the proton p-h energy gaps are $\sim$22 MeV and $\sim$28 MeV for states of negative and positive parity, respectively. Such a large gap explains the practical absence of proton p-h configurations in the low-energy phonons and also the upward energy shift of the theoretical dipole strength with respect to the region of observation.

In order to obtain a smoother HF level scheme it is necessary to replace the NNLO$_{\rm opt}$ with other versions of chiral potential. The NNLO$_{\rm sat}$ [77] seems to be a promising candidate. It includes explicitly the three-body contribution and improves the description of binding energies and nuclear radii as well [78]. According to our preliminary calculations, such a potential yields a considerably more compact HF spectrum.

ACKNOWLEDGMENTS

This work was partly supported by the Czech Science Foundation (Czech Republic) under Grant No. 16-16772S. Two of the authors (F.K. and P.V.) thank the INFN (Italy) for financial support. Highly appreciated was the access to computing and storage facilities provided by the Meta Centrum under Program No. LM2010005 and the CERIT-SC under the program Centre CERIT Scientific Cloud, part of the Operational Program Research and Development for Innovations, Reg. No. CZ.1.05/3.2.00/08.0144.

[1] P. Thirolf, B. Pritychenko, B. Brown, P. Cottle, M. Chromik, T. Glasmacher, G. Hackman, R. Ibbotson, K. Kemper, T. Otsuka *et al.*, Phys. Lett. B **485**, 16 (2000).

[2] A. Ozawa, T. Kobayashi, T. Suzuki, K. Yoshida, and I. Tanihata, Phys. Rev. Lett. **84**, 5493 (2000).

[3] M. Stanoiu, F. Azaiez, Z. Dombrádi, O. Sorlin, B. A. Brown, M. Belleguic, D. Sohler, M. G. Saint Laurent, M. J. Lopez-Jimenez, Y. E. Penionzhkevich *et al.*, Phys. Rev. C **69**, 034312 (2004).

[4] E. Becheva, Y. Blumenfeld, E. Khan, D. Beaumel, J. M. Daugas, F. Delaunay, C.-E. Demonchy, A. Drouart, M. Fallot, A. Gillibert *et al.*, Phys. Rev. Lett. **96**, 012501 (2006).

[5] S. Michimasa, S. Shimoura, H. Iwasaki, M. Tamaki, S. Ota, N. Aoi, H. Baba, N. Iwasa, S. Kanno, S. Kubono *et al.*, Phys. Lett. B **638**, 146 (2006).

[6] C. S. Sumithrarachchi, D. J. Morrissey, B. A. Brown, A. D. Davies, D. A. Davies, M. Fancina, E. Kwan, P. F. Mantica, M. Portillo, Y. Shimbara *et al.*, Phys. Rev. C **75**, 024305 (2007).

[7] A. Schiller, N. Frank, T. Baumann, D. Bazin, B. A. Brown, J. Brown, P. A. DeYoung, J. E. Finck, A. Gade, J. Hinnefeld *et al.*, Phys. Rev. Lett. **99**, 112501 (2007).

[8] Z. Elekes, Z. Dombrádi, N. Aoi, S. Bishop, Z. Fülöp, J. Gibelin, T. Gomi, Y. Hashimoto, N. Imai, N. Iwasa *et al.*, Phys. Rev. Lett. **98**, 102502 (2007).

[9] C. R. Hoffman, T. Baumann, D. Bazin, J. Brown, G. Christian, P. A. DeYoung, J. E. Finck, N. Frank, J. Hinnefeld, R. Howes *et al.*, Phys. Rev. Lett. **100**, 152502 (2008).

[10] M. Stanoiu, D. Sohler, O. Sorlin, F. Azaiez, Z. Dombrádi, B. A. Brown, M. Belleguic, C. Borcea, C. Bourgeois, Z. Dlouhy *et al.*, Phys. Rev. C **78**, 034315 (2008).

[11] D. Sohler, M. Stanoiu, Z. Dombrádi, F. Azaiez, B. A. Brown, M. G. Saint-Laurent, O. Sorlin, Y.-E. Penionzhkevich, N. L. Achouri, J. C. Angélique *et al.*, Phys. Rev. C **77**, 044303 (2008).

[12] R. Kanungo, C. Nociforo, A. Prochazka, T. Aumann, D. Boutin, D. Cortina-Gil, B. Davids, M. Diakaki, F. Farinon, H. Geissel *et al.*, Phys. Rev. Lett. **102**, 152501 (2009).

[13] C. R. Hoffman, T. Baumann, J. Brown, P. A. DeYoung, J. E. Finck, N. Frank, J. D. Hinnefeld, S. Mosby, W. A. Peters, W. F. Rogers *et al.*, Phys. Rev. C **83**, 031303(R) (2011).

[14] E. Lunderberg, P. A. DeYoung, Z. Kohley, H. Attanayake, T. Baumann, D. Bazin, G. Christian, D. Divaratne, S. M. Grimes, A. Haagsma *et al.*, Phys. Rev. Lett. **108**, 142503 (2012).

[15] M. S. Basunia, Nucl. Data Sheets **127**, 69 (2015).

[16] A. Leistenschneider, T. Aumann, K. Boretzky, D. Cortina, J. Cub, U. Datta Pramanik, W. Dostal, T. W. Elze, H. Emling, H. Geissel *et al.*, Phys. Rev. Lett. **86**, 5442 (2001).

[17] E. Tryggestad, T. Aumann, T. Baumann, D. Bazin, J. R. Beene, Y. Blumenfeld, B. A. Brown, M. Chartier, M. L. Halbert, P. Heckman *et al.*, Phys. Lett. B **541**, 52 (2002).

[18] E. Tryggestad, T. Baumann, P. Heckman, M. Thoennessen, T. Aumann, D. Bazin, Y. Blumenfeld, J. R. Beenec, T. A. Lewis, D. C. Radford *et al.*, Phys. Rev. C **67**, 064309 (2003).

[19] H. Sagawa and T. Suzuki, Phys. Rev. C **59**, 3116 (1999).

[20] D. Savran, T. Aumann, and A. Zilges, Prog. Part. Nucl. Phys. **70**, 210 (2013).

[21] A. Volya and V. Zelevinsky, Phys. Rev. Lett. **94**, 052501 (2005).

[22] T. Otsuka, T. Suzuki, J. D. Holt, A. Schwenk, and Y. Akaishi, Phys. Rev. Lett. **105**, 032501 (2010).

[23] A. Cipollone, C. Barbieri, and P. Navrátil, Phys. Rev. Lett. **111**, 062501 (2013).

[24] A. Cipollone, C. Barbieri, and P. Navrátil, Phys. Rev. C **92**, 014306 (2015).

[25] J. D. Holt, J. Menéndez, and A. Schwenk, Eur. Phys. J. A **49**, 39 (2013).

[26] J. R. Gour, P. Piecuch, M. Hjorth-Jensen, M. Wloch, and D. J. Dean, Phys. Rev. C **74**, 024310 (2006).

[27] G. Hagen, T. Papenbrock, D. J. Dean, M. Hjorth-Jensen, and B. Velamur Asokan, Phys. Rev. C **80**, 021306(R) (2009).

[28] G. Hagen, T. Papenbrock, and M. Hjorth-Jensen, Phys. Rev. Lett. **104**, 182501 (2010).

[29] O. Jensen, G. Hagen, M. Hjorth-Jensen, and J. S. Vaagen, Phys. Rev. C **83**, 021305(R) (2011).

[30] O. Jensen, G. Hagen, M. Hjorth-Jensen, B. A. Brown, and A. Gade, Phys. Rev. Lett. **107**, 032501 (2011).

[31] G. Hagen, M. Hjorth-Jensen, G. R. Jansen, R. Machleidt, and T. Papenbrock, Phys. Rev. Lett. **108**, 242501 (2012).

[32] G. R. Jansen, J. Engel, G. Hagen, P. Navratil, and A. Signoracci, Phys. Rev. Lett. **113**, 142502 (2014).

[33] S. Bacca, N. Barnea, G. Hagen, M. Miorelli, G. Orlandini, and T. Papenbrock, Phys. Rev. C **90**, 064619 (2014).

[34] F. Andreozzi, F. Knapp, N. Lo Iudice, A. Porrino, and J. Kvasil, Phys. Rev. C **75**, 044312 (2007).

[35] F. Andreozzi, F. Knapp, N. Lo Iudice, A. Porrino, and J. Kvasil, Phys. Rev. C **78**, 054308 (2008).

[36] D. Bianco, F. Knapp, N. Lo Iudice, F. Andreozzi, and A. Porrino, Phys. Rev. C **85**, 014313 (2012).

[37] G. De Gregorio, F. Knapp, N. Lo Iudice, and P. Veselý, Phys. Rev. C **93**, 044314 (2016).

[38] D. Bianco, F. Knapp, N. Lo Iudice, F. Andreozzi, A. Porrino, and P. Veselý, Phys. Rev. C **86**, 044327 (2012).

[39] F. Knapp, N. Lo Iudice, P. Veselý, F. Andreozzi, G. De Gregorio, and A. Porrino, Phys. Rev. C **90**, 014310 (2014).

[40] F. Knapp, N. Lo Iudice, P. Veselý, F. Andreozzi, G. De Gregorio, and A. Porrino, Phys. Rev. C **92**, 054315 (2015).

[41] G. De Gregorio, J. Herko, F. Knapp, N. Lo Iudice, and P. Veselý, Phys. Rev. C **95**, 024306 (2017).

[42] G. De Gregorio, F. Knapp, N. Lo Iudice, and P. Veselý, Phys. Rev. C **94**, 061301(R) (2016).

[43] G. De Gregorio, F. Knapp, N. Lo Iudice, and P. Veselý, Phys. Rev. C **95**, 034327 (2017).

[44] G. De Gregorio, F. Knapp, N. Lo Iudice, and P. Veselý, Phys. Scr. **92**, 074003 (2017).

[45] A. Bohr and B. R. Mottelson, *Nuclear Structure* (W. A. Benjamin, New York, 1975), Vol. 2.

[46] S. Lie, T. Engeland, and G. Dhall, Nucl. Phys. A **156**, 449 (1970).

[47] S. T. Hsieh and H. Horie, Nucl. Phys. A **151**, 243 (1970).

[48] A. P. Shukla and G. E. Brown, Nucl. Phys. A **112**, 296 (1968).

[49] S. Lie and T. Engeland, Nucl. Phys. A **267**, 123 (1976).

[50] H.-L. Ma, B.-G. Dong, Y.-L. Yan, H.-Q. Zhang, D.-Q. Yuan, S.-Y. Zhu, and X.-Z. Zhang, Phys. Rev. C **93**, 014317 (2016).

[51] C. Mahaux, P. F. Bortignon, R. A. Broglia, and C. H. Dasso, Phys. Rep. **120**, 1 (1985).

[52] G. Co', V. De Donno, M. Anguiano, R. N. Bernard, and A. M. Lallena, Phys. Rev. C **92**, 024314 (2015).

[53] J. Toivanen and J. Suhonen, Phys. Rev. C **57**, 1237 (1998).

[54] S. Mishev and V. V. Voronov, Phys. Rev. C **78**, 024310 (2008).

[55] M. Tohyama and P. Schuck, Phys. Rev. C **87**, 044316 (2013).

[56] K. Yoshida, Phys. Rev. C **79**, 054303 (2009).

[57] G. Colò, H. Sagawa, and P. F. Bortignon, Phys. Rev. C **82**, 064307 (2010).

[58] P. F. Bortignon, G. Colò, and H. Sagawa, J. Phys. G: Nucl. Part. Phys. **37**, 064013 (2010).

[59] K. Mizuyama, G. Colò, and E. Vigezzi, Phys. Rev. C **86**, 034318 (2012).

[60] L.-G. Cao, G. Colò, H. Sagawa, and P. F. Bortignon, Phys. Rev. C **89**, 044314 (2014).

[61] D. Tarpanov, J. Dobaczewski, J. Toivanen, and B. G. Carlsson, Phys. Rev. Lett. **113**, 252501 (2014).
[62] M. Baldo, P. F. Bortignon, G. Colò, D. Rizzo, and L. Sciacchitano, J. Phys. G: Nucl. Part. Phys. **42**, 085109 (2015).
[63] N. V. Gnezdilov, I. N. Borzov, E. E. Saperstein, and S. V. Tolokonnikov, Phys. Rev. C **89**, 034304 (2014).
[64] E. Litvinova and P. Ring, Phys. Rev. C **73**, 044328 (2006).
[65] E. V. Litvinova and A. V. Afanasjev, Phys. Rev. C **84**, 014305 (2011).
[66] E. Litvinova, Phys. Rev. C **85**, 021303(R) (2012).
[67] A. V. Afanasjev and E. Litvinova, Phys. Rev. C **92**, 044317 (2015).
[68] A. Ekström, G. Baardsen, C. Forssén, G. Hagen, M. Hjorth-Jensen, G. R. Jansen, R. Machleidt, W. Nazarewicz, T. Papenbrock, J. Sarich *et al.*, Phys. Rev. Lett. **110**, 192502 (2013).
[69] C. Yannouleas, Phys. Rev. C **35**, 1159 (1987).
[70] S. Drozdz, S. Nishizaki, J. Speth, and J. Wambach, Phys. Rep. **197**, 1 (1990).
[71] P. Papakonstantinou and R. Roth, Phys. Rev. C **81**, 024317 (2010).
[72] P. Papakonstantinou, Phys. Rev. C **90**, 024305 (2014).
[73] D. Gambacurta, F. Catara, M. Grasso, M. Sambataro, M. V. Andrés, and E. G. Lanza, Phys. Rev. C **93**, 024309 (2016).
[74] D. Bianco, F. Knapp, N. Lo Iudice, P. Veselý, F. Andreozzi, G. De Gregorio, and A. Porrino, J. Phys. G: Nucl. Part. Phys. **41**, 025109 (2014).
[75] E. Khan, N. Sandulescu, M. Grasso, and N. V. Giai, Phys. Rev. C **66**, 024309 (2002).
[76] V. De Donno, G. Co', M. Anguiano, and A. M. Lallena, Phys. Rev. C **95**, 054329 (2017).
[77] A. Ekström, G. R. Jansen, K. A. Wendt, G. Hagen, T. Papenbrock, B. D. Carlsson, C. Forssén, M. Hjorth-Jensen, P. Navrátil, and W. Nazarewicz, Phys. Rev. C **91**, 051301(R) (2015).
[78] V. Lapoux, V. Somà, C. Barbieri, H. Hergert, J. D. Holt, and S. R. Stroberg, Phys. Rev. Lett. **117**, 052501 (2016).